

Review

Single Particle Inductively Coupled Plasma Time-of-Flight Mass Spectrometry—A Powerful Tool for the Analysis of Nanoparticles in the Environment

Ziwei Meng ^{1,2,†}, Lingna Zheng ^{2,†}, Hao Fang ², Pu Yang ², Bing Wang ², Liang Li ^{1,*}, Meng Wang ^{2,*} 
and Weiyue Feng ²

¹ Hubei Key Laboratory of Plasma Chemistry and Advanced Materials, Key Laboratory for Green Chemical Process of Ministry Education, School of Materials Science and Engineering, Wuhan Institute of Technology, Wuhan 430205, China

² CAS Key Laboratory for Biomedical Effects of Nanomaterials and Nanosafety, CAS-HKU Joint Laboratory of Metallomics on Health and Environment, and Beijing Metallomics Facility, Institute of High Energy Physics, Chinese Academy of Sciences, Beijing 100049, China

* Correspondence: msell08@163.com (L.L.); wangmeng@ihep.ac.cn (M.W.)

† The authors contributed equally to this work.

Abstract: Single-particle inductively coupled plasma-mass spectrometry (SP-ICP-MS) has emerged as an important tool for the characterization of inorganic nanoparticles (NPs) in the environment. Although most SP-ICP-MS applications rely on the quadrupole ICP-MS (ICP-QMS), it is limited by the slow scanning speed of the quadrupole. Recent advancements in instrumentation have led to the development of inductively coupled plasma time-of-flight mass spectrometry (ICP-TOF-MS) which offers a viable solution. In this review, we discuss the recent advances in instrumentation and methodology of ICP-TOF-MS, followed by a detailed discussion of the applications of SP-ICP-TOFMS in analyzing NPs in the environment. SP-ICP-TOFMS has the potential to identify and quantify both anthropogenic and natural NPs in the environment, providing valuable insights into their occurrence, fate, behavior, and potential environmental risks.

Keywords: single particle analysis; ICP-TOFMS; nanoparticles



Citation: Meng, Z.; Zheng, L.; Fang, H.; Yang, P.; Wang, B.; Li, L.; Wang, M.; Feng, W. Single Particle Inductively Coupled Plasma Time-of-Flight Mass Spectrometry—A Powerful Tool for the Analysis of Nanoparticles in the Environment. *Processes* **2023**, *11*, 1237. <https://doi.org/10.3390/pr11041237>

Academic Editor: Ofelia Anjos

Received: 9 March 2023

Revised: 3 April 2023

Accepted: 5 April 2023

Published: 17 April 2023



Copyright: © 2023 by the authors. Licensee MDPI, Basel, Switzerland. This article is an open access article distributed under the terms and conditions of the Creative Commons Attribution (CC BY) license (<https://creativecommons.org/licenses/by/4.0/>).

1. Introduction

The widespread use of nanoparticles (NPs) in industry continues to pose threats to the environment and increase health risks to organisms [1,2]. The release of engineered NPs from industrial products (such as metal nanoparticles and carbon nano-tubes) inevitably results in human exposure to NPs and is increasing with the rapidly expanding production of engineered NPs [3]. In this context, controlling NP discharge, evaluating NP health risks, and developing new regulations on NPs depend on improving the current knowledge about the occurrence, fate, behavior, and potential risks of NPs in the environment [4]. Therefore, there is an urgent need for the development of innovative and reliable methods of NP analysis [5], which require increasingly sophisticated nanometrology capable of providing accurate and robust quantitation and characterization of NPs.

NPs are generally heterogeneous in size, composition, crystallinity, and surfaces, and these characteristics significantly impact the industrial performance and environmental fate of NPs. Although instrumentation and standardized methods have been developed for decades to examine nano-scale features [6,7], the laborious sample preparation and insufficient detection limits (e.g., much higher than the actual concentration of $\mu\text{g}\cdot\text{L}^{-1}$ in environmental samples) hinder reliable, accurate, and high-throughput analysis. Moreover, many of the available methods are not suitable for analyzing NPs in a real environmental sample with complex matrixes and interferences. Furthermore, there is even less characterization of individual nanoparticles, and analysis of NPs at a single particle level

continues to be a limiting factor for risk assessment and the development of NP pollution monitoring approaches.

To address the above challenges in analyzing NPs, inductively coupled plasma-mass spectrometry (ICP-MS) has been adapted to provide sensitive, element-specific, and high throughput single particle analysis [8]. ICP-MS involves desolvating, atomizing, and ionizing a sample in solution in the ion source of a high-temperature plasma (~6000 K) with the resulting ions analyzed by a mass analyzer [9]. By introducing a sufficiently diluted suspension of NPs into ICP-MS, only one particle is statistically introduced at a time. This transforms ICP-MS into a versatile technique with unique advantages that can provide information on the elemental composition, number concentration, and size distribution of NPs with mass concentrations down to the ng L^{-1} at a single particle level [10,11]. This technique is commonly referred to as single particle ICP-MS (SP-ICP-MS).

SP-ICP-MS has a high-throughput capability and relatively low running cost for single particle analysis and is considered an emerging tool for detecting and characterizing NPs in the environment. Initially, single particle analysis was carried out using inductively coupled plasma-optical emission spectroscopy (ICP-OES) [12]. Later, ICP-MS was introduced to improve the sensitivity and detection limits for single particle analysis [13–17]. The spectral interference in ICP-MS was a challenge, but it was addressed by using collision/reaction cell technology [18], a high-resolution mass analyzer [19], or a triple quadrupole ICP-MS (ICP-MS/MS) system [20,21].

Currently, most applications of SP-ICP-MS rely on the quadrupole ICP-MS (ICP-QMS). It is important to note that scanning-type mass analyzers (e.g., a quadrupole) can only monitor ions with a single m/z ratio at a time [22,23]. However, both anthropogenic and natural NPs in the real world are complex when found in water [24,25], soil [26,27], and indoor dust [28], often containing multiple elements. Moreover, NPs become even more complex after undergoing chemical and physical transformations due to interactions with environmental matter. Therefore, multi-element analysis in SP-ICP-MS is crucial for the comprehensive characterization of NPs in real-world samples.

Inductively coupled plasma time-of-flight mass spectrometry (ICP-TOFMS) allows for multi-element analysis in a short time period, thus making it a promising tool for the analysis of NPs in real-world samples [29–32]. TOFMS was first combined with an ICP in the early 1990s [33] and, after several decades of development, it has achieved better detection limits and analytical speed. The new generation of ICP-TOFMS can determine the entire mass spectrum (usually from 7 to 275 Th) in tens of microseconds, enabling the analysis of multi-elements in a single NP [34,35].

This review will describe recent advances in the instrumentation and methodology of ICP-TOF-MS, followed by a detailed discussion of the applications of SP-ICP-TOFMS in analyzing NPs in the environment. The future prospects of SP-ICP-TOFMS methods and applications will also be discussed.

2. SP-ICP-TOFMS: Instrumentation and Methodology

2.1. TOF Analyser for Single Particle Analysis

SP-ICP-MS has become a widely used and routine tool in many fields [28,36–38]. Commercial instruments typically use one of the following mass analyzers: quadrupole (Q), sector field (SF), or time-of-flight (TOF). For the ICP-MS equipped with a scanning mass analyzer, fast and continuous switching between different m/z channels is required for monitoring a transit signal [31]. The settling time and dwell time are key parameters for the accurate analysis of NPs. The dwell time is the time required to measure a single m/z value in a single run while the settling time is the time required for the analyzers to stabilize for the measurement of the next m/z value. Due to the short duration of a single particle in the plasma (usually a few hundred microseconds [6]), it is hard to detect more than one or two isotopes per NP in a single run, even using the shortest dwell time and settling time in the modern quadrupole ICP-MS [39].

To improve the accuracy of particle analysis, the signal can be elongated to several milliseconds using collision cell technology to achieve the accurate and precise analysis of more than one isotope in a single NP [40]. Multi-collector ICP-MS(MC-ICP-MS) is an alternative technique to the multi-element analysis of a single NP due to its capability to simultaneously monitor multiple isotopes [41]. Equipped with a fast detector (e.g., a multichannel ion counter), MC-ICP-MS achieves the simultaneous acquisition of several isotopes with a very short dwell time (e.g., 30 μ s [42]), making it a powerful tool for the multi-element analysis of a single NP. However, when analyzing NPs with more complex elements, only a limited number of isotopes within a restricted mass range can be detected. If the sample is unknown, the target elements must be screened first, followed by targeted analysis, which may reduce sample utilization rates.

In contrast to the above mass analyzers, time-of-flight (TOF) mass analyzers provide a quasi-simultaneous detection of all elements and have great advantages for multi-element and high throughput analysis of single particles. Commercial TOF mass spectrometry was introduced in the 1950s and its outstanding features have been confirmed. The principle of TOFMS involves generating ions, followed by ion acceleration, and measuring the flight time of ions in a drift tube. During the process, all ions acquire the same kinetic energy in the acceleration region, with differences in velocity arising from variations in mass-to-charge. If the flight distance is known, it is possible to determine the mass-to-charge ratio of the ions by measuring the flight time of the ions, as demonstrated in Equations (1) and (2):

$$v = \sqrt{\frac{2zeV}{m}} \quad (1)$$

$$t = \frac{L}{v} = \sqrt{\frac{m}{2zeV}} \cdot L \quad (2)$$

where v is the speed of an ion; z is the charge of the ion; e is the electron charge; V is the acceleration voltage; m is the mass of the ion; t is the flight time; and L is the flight distance of the ion.

In a commercial ICP-TOFMS, the heaviest ions reach the detector in the tens of microseconds, which means that a few full mass scans can be completed for a transit signal from a single NP [43]. A new generation of ICP-TOFMS instruments is currently on the market, including the icpTOF from TOFWERK, Vitesse from Nu Instruments, and CyTOF from Standard BioTools (formerly known as Fluidigm). These instruments use the same orthogonal design and single-pass reflectron TOF design. With a fast acquisition speed (i.e., 30 μ s for one TOF full mass spectrum extractions [34]), ICP-TOFMS can determine multi-elements in a single NP and become a promising technique for single cell analysis and single particle analysis [6,44,45].

2.2. Sample Introduction Systems for Single Particle Analysis

The sample introduction system is regarded as the Achilles' heel of ICP-MS. A standard sample introduction system contains a chamber and a nebulizer with a typical transport efficiency of less than 5%, which decreases with an increase in the sample uptake rate [46]. However, by using a modified sample introduction system with a single-pass chamber and a low-consumption nebulizer, transportation efficiency can be improved [47]. For example, Tharaud et al. achieved ~100% transport efficiency by using a direct injection high-efficiency nebulizer [48].

Standard sample introduction systems generate polydisperse aerosols that lead to an inaccurate analysis with SP-ICP-MS due to different ionization processes and sampling biases that NPs undergo. Moreover, standard sample introduction systems often suffer from severe matrix effects. To address these issues, monodisperse droplets generated by either a commercial piezoelectric dispenser [49] or a microfluidics-based droplet dispenser [50] have been used to create a better sample introduction method. Hendriks et al. demonstrated that

the microdroplets generated by an online introduction system can be used as an accurate and matrix-independent calibration for single particle analysis with SP-ICP-TOFMS [51].

In addition to solution analysis, in situ solid sampling can be achieved using laser ablation (LA) as a sample introduction system. In LA-ICP-MS analysis, solid samples are ablated by high-power laser shots, and the resulting aerosols are transported and analyzed by ICP-MS. When the laser fluence is attenuated at a suitable level, LA-ICP-MS could be used as a sensitive tool for analyzing and imaging NPs as the intact NPs are transported into the ion source by a carrier gas. This method provides in situ information on particle size and number. Metarapi et al. used LA-SP-ICP-MS to image and discriminate silver NPs (AgNPs) and silver ions in sunflower roots [52]. Additionally, Wang et al. imaged AgNPs and released Ag ions in the organs of mice exposed to AgNPs using LA-SP-ICP-MS, providing a valuable tool to study the uptake, translocation, and degradation characteristics of NPs in organisms [53].

The sample introduction system is crucial for successful SP-ICP-MS analysis, and different sample introduction methods are gradually overcoming the challenges faced by standard methods [48,51]. Together with recent developments in TOF instrumentation, the sample introduction systems make it more feasible to analyze single particles by ICP-TOFMS.

2.3. Identification of NPs from Backgrounds

The complexity of signals in SP-ICP-MS surpasses that of traditional ICP-MS solution analysis. In SP-ICP-MS, a single particle is statistically introduced into the plasma at a time, producing an ion cloud that represents the elemental composition of the particle. The ion cloud is then passed through the ion optics and mass analyzer, resulting in a transient signal with typical durations between 300 and 1000 μs [6,54,55]. Separating the transient signal from the steady-state background is a critical aspect of SP-ICP-MS. An accurate measurement of the size and concentration of NPs is only possible if the NP signal can be distinguished from the background signal.

The most common strategy for detecting NPs in SP-ICP-MS is to treat NP signals as outliers from background signals. An iterative algorithm is used to discriminate a NP from the dissolved background when the NP signal exceeds the critical value (L_C), as shown in Equation (3) [56–58].

$$L_C = n\sigma_b \quad (3)$$

where L_C is the critical value; σ_b is the standard deviation of the background; n is the abscissa of the standardized normal distribution defined by false-positive errors (α).

There is no agreement on the value of n , and different values are found in the literature, typically ranging from 3σ [59,60] to 5σ [59,61,62]. It should be noted that the n - σ threshold method assumes that the background signals in SP-ICP-MS follow a Gaussian distribution.

Some researchers have also developed critical value approaches based on Poisson-distributed background signals [5]. As defined by Currie [63] and adopted by IUPAC [64], there are two detection criteria: the critical value (L_C , the minimum detectable signal) and the detection limit (L_D , the minimum signal level that results in reliably detected signals), which are defined by false-positive errors (α) and false-negative errors (β) [65]. Poisson distributions show a significant asymmetry for the low values of its mean. The typical value usually used for α and β is 0.05 as shown in Equations (4) and (5) [63].

$$L_C = 1.64\sqrt{\lambda_b} \quad (\alpha = 0.05) \quad (4)$$

$$L_D = 2.71 + 3.29\sqrt{\lambda_b} \quad (\alpha = 0.05, \beta = 0.05) \quad (5)$$

where λ_b is the average count rate of the background signal.

However, the shape of mass spectrometric signals obtained by an analog-to-digital conversion (ADC) with high-speed digitizers in modern ICP-TOFMS instruments often does not follow a Gaussian distribution, especially for low-count signals [65,66]. This is because the use of such high-speed digitizers increases the variance from Poisson noise

and causes the output signals of an electron multiplier detector to have a distribution (i.e., the pulse-height distribution, PHD) [65]. In this case, the shape of ICP-TOFMS signals can be described by a compound Poisson distribution of the measured PHD of the detector and a Poisson distributed ion arrival at the detector [65,66]. Gundlach-Graham et al. developed a Monte Carlo simulation of the TOF signals of single particle analysis by ICP-TOFMS. They proposed a new method to calculate L_C and L_D , which is used as the threshold for single particle analysis by ICP-TOFMS. The new α and β values are 0.001 and 0.05, respectively [65]. As shown in Equations (6) and (7)

$$L_C = \lambda_b + 3.41\sqrt{\lambda_b} + 1.6 \quad (\alpha = 0.001) \quad (6)$$

$$L_D = \lambda_b + 5.24\sqrt{\lambda_b} + 5.54 \quad (\alpha = 0.001, \beta = 0.05) \quad (7)$$

where λ_b is the average count rate of the background signal.

This new method can effectively separate the overlapping background from NP distributions, resulting in a more accurate detection threshold and size measurement of NPs [65]. Moreover, it can be applied to other mass spectrometers that are equipped with electron multiplier detectors and fast digitizers.

2.4. Quantification for SP-ICP-TOFMS

Calibration is an essential step in SP-ICP-TOFMS, as it enables the accurate and quantitative analysis of NPs in solution. In SP-ICP-TOFMS, the intensity of NP signals is proportional to the mass of the NPs, and the number of events detected is proportional to the number of NPs in the sample solution. Currently, many methods are used for quantitative analysis by SP-ICP-MS [5,45].

The first quantitative method involves utilizing NP standard materials to establish a functional relationship between the particle size and signal response. However, the lack of standard NP materials of similar composition, shape, and size as those of NP samples limits its applicability.

The second quantitative method, widely used by researchers, relies on the calibration curve of a standard solution and the measurement of transport efficiency. This method assumes that the ionization efficiency difference between the standard solution and NPs can be disregarded, which is generally true. To achieve accurate quantification, measuring the transport efficiency (η_{neb}) is crucial. Three methods have been proposed for measuring transport efficiency, including the waste collection, particle frequency, and particle size methods [57].

The waste collection method indirectly determines transport efficiency by collecting the waste solution out of the spray chamber and calculating the actual amount of analyte entering the ICP-MS. However, this method may overestimate transport efficiency due to the presence of water vapor and residual liquid in the spray chamber [57]. The particle frequency method calculates transport efficiency by dividing the number of detected events by the total number of NPs sampled during the data acquisition time. However, determining the accurate concentration of NPs is challenging due to the lack of NP standard materials and potential NP aggregation. The particle size method involves comparing the sensitivity of an element in NPs with that obtained from the standard solution of the same element. The transport efficiency can be calculated by dividing the two sensitivities. Many studies show that the particle size method provides superior accuracy [45]. However, if there is a difference in the ionization efficiency of the NPs and standard solutions, it may introduce additional errors [67].

The two quantitative methods mentioned above do not fully utilize the benefits of the full-element analytical capability available with SP-ICP-TOFMS. The third quantitative method is the use of monodisperse microdroplets as quantitative standards of NPs [68,69]. This method, illustrated in Figure 1 [70], uses a two-sample introduction system where a microdroplet containing a known element concentration is merged into an aerosol produced

by a pneumatic nebulizer and then introduced into the ICP-TOFMS. The online microdroplet calibration technique offers an automatic matrix-matching calibration of signals from individual NPs [51,71]. Mehrabi et al. determined the size and concentration of NPs by the online microdroplet calibration method while accounting for matrix effects in the single particle analysis in a single step [70]. Harycki et al. conducted a study to evaluate the effectiveness of online microdroplet calibration for quantifying nanoparticles in three organic matrices—ethanol, acetone, and acetonitrile. Despite these matrices causing signal attenuation up to 35 times and having a nebulizer transport efficiency 4 times higher than pure water matrices, the NP sizes and particle number concentration (PNC) in the organic matrices were determined with 98% accuracy [72].

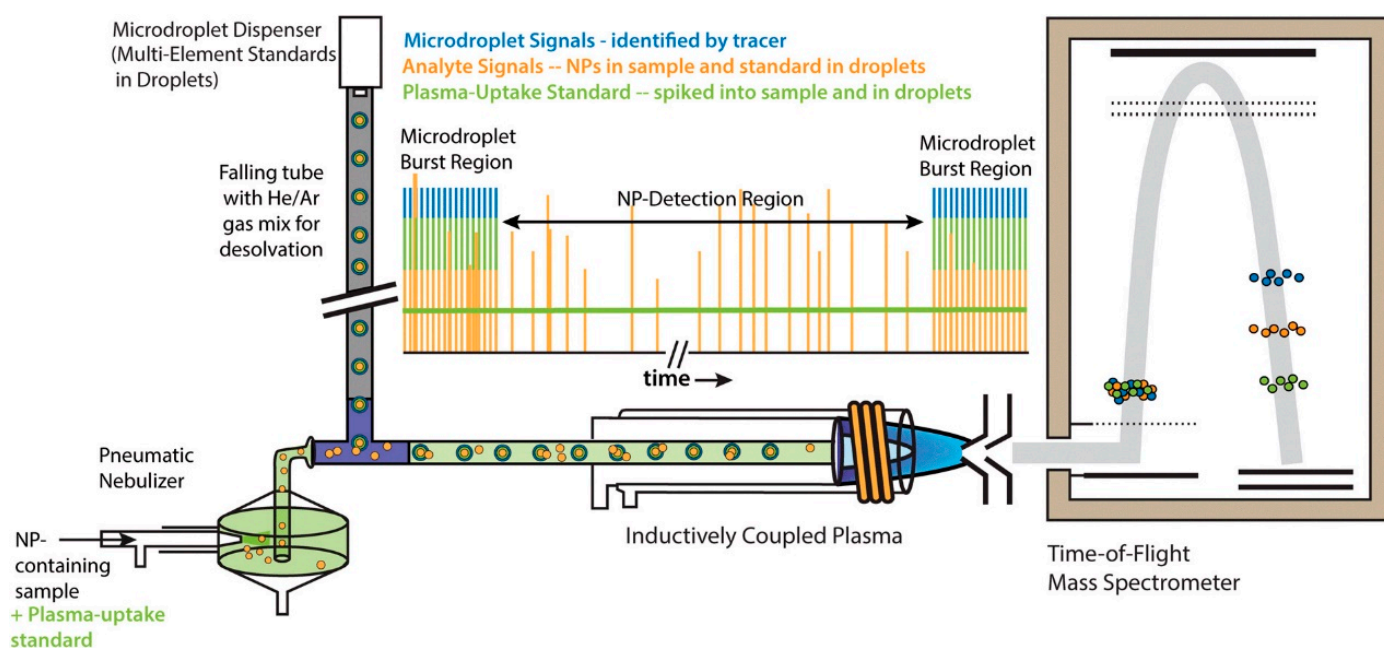


Figure 1. Schematic diagram of the online microdroplet calibration approach. Microdroplets composed of multi-element solutions are introduced into the ICP to provide absolute sensitivities ($\text{counts} \cdot \text{g}^{-1}$) for the calibration of NP mass. The droplet signals are measured in the “Microdroplet Burst Regions” of the TOF time trace. At the same time, NP-containing samples are introduced into the ICP via conventional pneumatic nebulization. NP signals are analyzed from the “sp-Region” of the TOF time trace, which typically lasts a few minutes in duration. Through the addition of a known amount of plasma uptake standard to both nebulized samples and microdroplet standards, the plasma uptake rate is determined in each analysis, which is then used to calibrate the PNC. The plasma uptake standard is usually Cs (Reprint with permission from Kamyar M. Environ. Sci.: Nano. 2019, 6, 3349–3358. Copyright 2019, Royal Society of Chemistry [70]).

Compared to other single-particle calibration methods, the microdroplet calibration method offers the advantage of the elimination of matrix effects. In addition, mass quantification is not reliant on measuring the sample transfer efficiency. Furthermore, the mass is calibrated for each particle measurement, compensating for the instrument drift and other possible negative effects during a long run.

3. SP-ICP-TOFMS: Applications

3.1. Simultaneous Quantification of Multiple Elements in a Single Particle

SP-ICP-TOFMS is a promising approach that enables the multiplexed detection and quantification of diverse metal and metal-oxide NPs [35]. ICP-TOFMS is non-targeted multi-element measurement that allows the quantification of individual particles, enabling the accurate measurement of high-throughput and in situ multi-elements. For diverse environmental samples, SP-ICP-MS still has the potential to measure real environmental

samples at a level of 10^2 – 10^6 NPs·mL⁻¹ [73]. This method is practical for quantifying natural and anthropogenic nanoparticles in complex or unclear environmental matrices, which is critical for the ecotoxicological risk assessment of NPs, including engineered nanoparticles and natural nanoparticles [74–76].

The complexity of their composition and structure makes it difficult to determine the properties of NPs. At present, the research on composite nanoparticles mainly focuses on the core/shell structure of spherical nanoparticles with an uneven distribution of element components. Au in core and Ag in shell structure has usually been used for the evaluation of multi-element accuracy [66]. Generally, the measurement sensitivity of these elements is relatively high without much interference [29]. However, their behavior cannot be generalized and extrapolated to other composite nanoparticles, such as nano-steel (a Fe, Cr, Ni, Mo alloy used in composites) and bismuth vanadate particles (BiVO₄) [77,78]. Naasz et al. [31] provided a systematic and critical evaluation of the performance of ICP-TOFMS and ICP-QMS instruments for the analysis of nanoparticles used in a variety of industrial applications with complex structures and compositions. They found that only SP-ICP-TOFMS can accurately assess the elemental composition of nano-steel particles. Erhardt et al. achieved full element quantification of ice core samples in the environment by a combination of SP-ICP-TOFMS with continuous flow analysis [79]. This setup allows for accurately measuring target element concentrations over the entire mass range without losing sensitivity as the number of analytes increases.

Different elemental compositions on a single particle can often indicate the source of the particle. Multi-element analysis by SP-ICP-TOFMS has been applied to more complex samples such as air samples (e.g., road dust [80], samples from the International Space Station [81], and biomass-burning aerosol and ash [82]), water samples (e.g., wastewater [83] and rainfall [84]), and geological samples (e.g., soil [30] and minerals [32]). These applications provide guidelines for exploring how trace elements are transported into the environment. In addition, SP-ICP-TOFMS is expected to be used in medical research. Nanoparticles are increasingly used in medical products and devices, and their properties are critical for such applications. Recently, Mehrabi et al. detected magnetic iron nanoparticles by SP-ICP-TOFMS and applied it to a case study of magnetic filtering medical devices. Magnetic filtration was shown to reduce the mass concentration of detectable C/Fe₃C NPs by $99.99 \pm 0.01\%$ in water [85].

For many analytical techniques, it is difficult to assign the particle type in a sample that contains mixtures of NPs with similar major and minor element compositions. The elemental composition of a single particle can provide much information, especially in the environment. For example, the origin of Ce-NPs is related to the presence of other rare earth elements. Based on this characteristic, Szakas et al. reported a new class of anthropogenic accidental Ce-NPs, which cannot be distinguished from natural Ce-NPs by the previous binary classification approach [86].

Another major challenge is to distinguish and quantify anthropogenic particles from naturally occurring particles [1]. The unknown multi-element NPs constitute the bulk of accidental particles as the sources are often composed of many complex elements (e.g., brake and tire wear [87]). Particles from different regions have different elemental compositions that form specific clusters, which is called “elemental fingerprints”. Elemental fingerprinting can be used for tracing and migration clustering of particulate matter [82,83]. Due to elemental complexity, the need for the analysis and integration of data generated by SP-ICP-TOFMS is gradually increasing. There is no complete inventory of commercial or industrial-engineered NPs, and few data are available on the abundance of natural NPs. Establishing inventories of engineered and natural NPs depends on the development of high-throughput analytical methods. SP-ICP-TOFMS provides a direct way to build such databases.

For the huge data obtained by SP-ICP-TOFMS, some studies have developed new datum processing methods. Baalousha et al. characterized soil NPs at the single particle level in order to determine the purity, composition, association, and ratio of the elements in

the NPs [88]. To identify unique metallic fingerprints in natural NPs, cluster analysis was performed using MATLAB to identify clusters/groups of natural nanoparticles with similar elemental composition and to determine their average elemental composition. This method has also been applied to the element cluster analysis of mineral dust aerosols [89]. In addition, Mehrabi et al. proposed a method that employed automated single-nanoparticle quantification and classification for an unsupervised clustering analysis of multi-metal NPs to identify unique classes of NPs based on their element compositions [83,90]. Furthermore, Holbrook et al. built a machine-learning model using Pearson correlations and unsupervised t-distributed stochastic neighbor embedding (t-SNE) to find patterns of co-occurring elements and attribute possible particle sources based on the values reported in the literature [91]. As shown in Figure 2, Pearson correlations were used to find trends in element correlations, and t-SNE projects the high-dimensional dataset (a 25-element feature set with a 1–4 element dimension target) into a lower-dimensional space of 2 dimensions [91]. The factor that often has the strongest impact is the perplexity argument in t-SNE analysis, which was tested using values of 5, 30, and 50 by the author. The performance of the data result is the space between apparent clusters and data points (a value of 30 was chosen for these samples, as shown in Figure 2B). The information obtained from the correlation and t-SNE analysis was combined with the reported document element tags to create an efficient data processing pipeline using the LightGBM multi-class classifier.

The machine learning model ultimately automates the dataset labeling and classification work, providing a fast and efficient method for inter/intra sample comparison in terms of multi-element NP elemental correlations. The pipeline can be further developed in the future to fully automate the analysis process for large particle datasets. In addition, a binomial logistic regression (LR) written by Bland et al. used the Python Sci-Kit learning module to compile a binomial LR combined with the SP-ICP-MS dataset to discriminate engineered titanium dioxide nanomaterials from natural titanium nanomaterials in soil [26]. Table 1 shows the selected applications of SP-ICP-TOFMS.

Table 1. The selected applications of SP(SC)-ICP-TOFMS.

| ICP-TOFMS Instrument | Sample Type | Sample Treatment | Sample Introduction System | Key Elements to Observe | Main Conclusion | Ref. |
|----------------------|---|---|---|---|---|------|
| Prototype icpTOF | CeO ₂ ENPs and CeO ₂ NNPs in soil | Colloid extraction procedure | Pneumatic nebulizer and cyclonic spray chamber | CeO ₂ ENPs, elemental fingerprint (Ce/La) associated with Ce-containing NNPs | CeO ₂ ENPs and Ce-NNPs were found to have elemental associations with La, Nd, and Th. CeO ₂ ENPs could be quantified in the matrix of Ce-NNPs based on multi-element NP element fingerprinting. | [30] |
| icpTOF R | TiO ₂ ENPs and TiO ₂ NNPs in lake water | Centrifugation to remove large particles, sonication, shaking in vortex, and dialysis | NC | Ti/Al, Ti/Mn, Ti/Fe, Ti/Pb, and Fe/Pb in a single particle | TiO ₂ ENPs, Ti-containing NNPs, and associations with Al, Mn, Fe, and Pb have been proposed as indicators of Ti-NNPs. | [92] |
| icpTOF R | Polar ice ice-core sample | Combined with Continuous flow analysis, the ice was melted and introduced | Bern CFA system, micro mist, and glass expansion | Element ratio in Fe-containing NNPs (Mg/Al, Fe/Al, and Mg/Fe) | ICP-TOFMS improved the resolution of the CFA; the iron-bearing aerosol concentration covaried with atmospheric particulate dust concentration. Further evidence of particle traceability was provided by the isotope. | [79] |
| icpTOF R | Steels | Dilution, acid treatment, sonication, centrifugation, and redispersion | Pneumatic nebulizer and cyclonic spray chamber | Ti and Nb | Quantified TiCN, NbCN, and TiNbCN NNPs. | [93] |
| icpTOF R | NPs in a heavy metal matrix, acid, and PBS matrix | Dilution and sonication | PFA MicroFlow pneumatic nebulizer, double pass cyclonic spray chamber, and microdroplet generator | Cs, Au, and Ag isotope | The study focused on the accurate calibration of NP size in various matrices using an online microdroplet calibration. | [51] |
| icpTOF 2R | River and urban runoff | Dilution, and sonication | PFA MicroFlow pneumatic nebulizer and quartz cyclonic spray chamber | Zn, with Fe, Mn, Al, and Si | The multiple elements in each particle were quantified and tracked. It was possible to develop the basis of the field of particle-by-particle geology. | [94] |
| Vitesse | Runoff from outdoor stains and paints | Sonication and filtration | NC | TiO ₂ , Al, Si, Fe, Zr, and Ce | TiO ₂ ENPs and Ti-NNPs associated with Al, Si, Fe, Zr, and Ce were proposed to indicate the assignment of particles as Ti-NNP. | [95] |
| icpTOF R | Biomass-burning aerosol and ash | Dilution and filtration | PFA MicroFlow pneumatic nebulizer and cyclonic spray chamber | Zn, Al, Si, Fe | The source of burned biomass was discussed. The source of burned biomass Zn and other crustal elements after biomass burning were more likely to be present in ash than in the biomass burning aerosol. | [82] |

Table 1. Cont.

| ICP-TOFMS Instrument | Sample Type | Sample Treatment | Sample Introduction System | Key Elements to Observe | Main Conclusion | Ref. |
|----------------------|--|---|--|---|--|----------|
| icpTOF R | Topsoil samples from the surface to 15 cm below the surface | Wet sieve (45 µm), freeze-drying, dilution, and extraction by tetrasodium pyrophosphate | MicroFlow PFA pneumatic nebulizer and cyclonic spray chamber | Al, Fe, Ti, Si, Ce, Zr, Zn, Sb, and Sn | The elemental composition and associations of natural nanomaterials were analyzed at the single-particle level. Clustering analysis was used to distinguish NNPs. This study provided a methodology and baseline information on NNPs that can be used to differentiate NNPs from ENPs in environmental systems. | [88] |
| icpTOF R | Sedimentation basin, road dust, and tunnel road dust | Cloud point extraction and applied to slide | Microflow PFA pneumatic nebulizer and quartz cyclonic spray chamber | Cu, Zn, Sr, Y, Zr, Nb, Rh, Ru, Pd, Sn, Sb, Ba, La, Ce, Pr, Nd, Sm, Eu, Gd, Dy, Lu, Hf, Pt, Au, and Pb | Machine learning was developed to label and classify particle samples, providing a fast and effective method for inter- and intra-sample comparisons based on multi-element particle correlations. | [91] |
| icpTOF R | Vacuum bag dust samples collected from the International Space Station (ISS) | Dilution, resting, filtration, cleaning with compressed air, and redispersion | Pneumatic nebulizer and cyclonic spray chamber | Zr, Al, Ti, Fe, Ag, Pb, Mo, Cu, Sn, Ni, and Cr | The particle populations composed of different elements in the ISS and their sources were analyzed. | [81] |
| icpTOF 2R | WWTPs in Switzerland | Sonication, stewing, and dilution for the top sample | MicroFlow pneumatic nebulizer and PFA T-piece baffled cyclonic spray chamber/microdroplet generator | All elements | The continued development of elemental fingerprints to achieve the automatic quantification and classification of individual particles. Total element screening and single particle fingerprinting were found to effectively avoid the false results caused by the complex samples of inorganic particles containing organic compounds. | [83, 90] |
| icpTOF R | NbCN, TiNbCN extracted by steel, and ENPs in soil | Sonication, dilution in ultrahigh purity water | Pneumatic nebulizer and cyclonic spray chamber | All elements | TiO ₂ was used as a tracer to monitor urban runoff. The study found that naturally occurring particles had the same elemental ratios and origin. After cells were stained with Ru red, it was found that the Ru content was directly related to cell volume, and cell size could be calculated by combining it with known cell shapes, leading to the calculation of the concentration of the target element in individual cells. | [27] |
| icpTOF R | Surface waters following rainfall | Well-shaking, sonication, and centrifugation to remove large particles | Pneumatic nebulizer and cyclonic spray chamber | Ti, Nb, Ce, and La | The concentrations of Ti-, Ce-, and Ag-containing NNPs were presented for both surface waters and precipitation. The origin was determined from the size and composition of the nanoparticles. | [84] |
| icpTOF R | Yeast cells and algal cells | Dilution in Milli Q water | NC | Mg, P, Ru, Ca, and Fe | Using the online isotope dilution analysis method, particles were characterized with a ¹⁹⁴ Pt/ ¹⁹⁵ Pt ratio while monitoring ¹⁸² W/ ¹⁸³ W for mass bias correction, allowing an accurate quantification at a high matrix concentration. | [96] |
| Vitesse | Global surface waters and precipitation | Sonication and filtration | Aridus II desolator | Ti, Ce, and Ag | Machine learning models of elemental fingerprinting and mass distribution were used to identify TiO ₂ ENPs and NNPs in soil; this method effectively reduced the effect of a high matrix. | [97] |
| icpTOF 2R | Pt NNPs | Leached with diluted nitric acid and dilution | Microdroplet generator introduction, control, and autosampler system | Pt isotope and W isotope | This study is to evaluate the traceability of isotopically enriched ENPs at the individual particle level in soil and provides guidance on the isotope enrichment requirements for the quantification of ENPs from earth-abundant elements in soils. | [98] |
| icpTOF R | Soil spiked TiO ₂ | <500 nm particle extraction from soil and sludge, enrichment with cloud point extraction, and dilution for analysis | Concentric borosilicate glass nebulizer and baffled cyclonic, high-purity quartz spray chamber | Ti, Ce, Ba, Rb, Fe, Mg, Mn, Nb, Pb, and other earth-abundant elements | The GSR particles were classified and their particle size was determined. In addition, the composition of the GSR particles was analyzed. | [26] |
| icpTOF R | Soil | Same as the last one | Concentric borosilicate glass nebulizer and baffled cyclonic, high-purity quartz spray chamber | Ti isotope | The particle size and composition of MDAs in wet deposits could be effectively analyzed by SP-ICP-TOFMS, but the quantification of the particle number has a greater uncertainty. The characterization of nanoscale MDAs can be used to better understand particle dynamics in the atmosphere. | [99] |
| icpTOF 2R | Gunshot residues | Settling to remove large particles and collecting the suspension's surface | PFA MicroFlow pneumatic nebulizer and quartz cyclonic spray chamber | Mg-U (65 species) | TiO ₂ NNPs in the organic matrix were accurately quantified by using the online microdroplet calibration method. | [100] |
| icpTOF S2 | Nano-scale mineral dust aerosols (MDAs) in snow | Sonication and filtration | Micro FAST MC autosampler, PFA pneumatic nebulizer, and cyclonic spray chamber | Al, Ti, Mn, Fe, Cu, Zn, Y, Zr, Nb, La, Ce, Nd, Pb, Th, and U | Low m/z detection capabilities were explored by analyzing carbon and metals in both microdroplets and uniform polystyrene (PS) beads. | [89] |
| icpTOF S2 | TiO ₂ in organic matrices | Sonication and dilution in ultrapure water | PFA MicroFlow pneumatic nebulizer and piezoelectric droplet generator cyclonic spray chamber | Cs and Ti | Bimetallic physical mixtures (CuAg + CuPd) could be distinguished from multi-metallic NNPs. Nanoscale structures relevant to bulk phenomena could be easily quantified and characterized with ensemble-representative reliability. | [72] |
| icpTOF S2 | Microplastic containing metals | Aqueous dispersions | Cyclonic spray chamber, quartz nebulizer with nanoparticle measurement, and pneumatic nebulizer with an autosampler for microplastic measurement and microdroplet introduction | C, Ag, Au, Ce, Eu, Ho, and Lu | By analyzing the NP mass distributions, the study showed the effect of NP surface modification on the aggregation of C/Fe ₃ C NNPs in whole blood. Magnetic filtration was able to significantly reduce detectable particles in water. | [101] |
| icpTOF R | Anisotropic copper crystals | Dilution | Microdroplet introduction | Cu, Au, Ag, and Pd | | [102] |
| icpTOF 2R | C/Fe ₃ C NNPs in whole blood | 10 ⁶ × dilution | Pneumatic nebulizer and cyclonic spray chamber | Cr, Fe, and Ce | | [85] |

Table 1. Cont.

| ICP-TOFMS Instrument | Sample Type | Sample Treatment | Sample Introduction System | Key Elements to Observe | Main Conclusion | Ref. |
|----------------------|---|---|--|--|---|-------|
| icpTOF 2R | River and its surrounding tributaries | Soaking with diluted nitric acid, rinsing with Milli-Q water, and filtration | Quartz cyclonic spray chamber | Si, Al, Fe, Pb, Mn, and Ce | Major element distributions showed diverse mineral populations. The elemental symbiosis of Ce/La and symbiosis of Fe, Mn, and Pb were found. | [32] |
| icpTOF 2R | Pb NPs were added to lake sediment (LDSK) samples | Centrifugation and colloid extraction procedure | Concentric pneumatic nebulizer combined with a membrane desolvation unit | Pb, Fe, Mg, Mn, Pb, and Zn | The SP-ICP-TOFMS method was developed to extract Pt NPs from LDSK, and its multi-element analysis was used to analyze the symbiotic elements of Pt in LDSK. | [103] |
| icpTOF 2R | Ag NPs and algal cells exposed to Ag NPs | Centrifugation and dilution | PFA MicroFlow pneumatic nebulizer and quartz cyclonic spray chamber | Ag isotope | The ability to monitor AgNPs and intracellular silver isotope ratios was investigated. | [104] |
| icpTOF R | Road dust particles | Sieving to remove large particles, well-dispersed with tube rotator, centrifugation, and top suspension collected | MicroFlow PFA pneumatic nebulizer and cyclonic spray chamber | Al, Ti, V, Cr, Fe, Co, Ni, Cu, Zn, Sn, Ce, Zr, Pb, and W | Samples were analyzed for total metal concentrations, particle elemental composition and ratios, and clustering. The study provided a reliable comprehensive approach to the characterization of road dust particles. | [80] |
| icpTOF 2R | Yeast cells | Any consequent dilutions before the injections | Quartz cyclonic spray chamber and SC-175 nebulizer | P and Pb | Coupling Asymmetric Flow Field Fractionation (AF4) with SC-ICP-TOFMS effectively removes the influence of heavy metal ions in the mass spectrum and simplifies the sample analysis process. | [105] |
| CyTOF | Intrahepatic and peripheral natural killer (NK) cells | Enzymatical digestion, filtration, and density gradient centrifugation | NC | 32 species transition-metal elements | Revealed the landscape of NK cell phenotypes in HCC patients to find potential immunotherapy targets by profiling the status of 32 surface markers in individual healthy and hepatocarcinoma cells. | [106] |
| CyTOF | Human immune cells, stem cells, and tumor cells | Antibody labeling | NC | ¹⁹⁴ Pt, ¹⁹⁵ Pt, ¹⁹⁶ Pt, ¹⁹⁸ Pt, ¹¹⁵ In, ¹¹³ In, and Pd | Metallic antibodies were used to label cells and a live cell barcode was established for the analysis of samples containing heterogeneous populations, such as mixtures of tumor cells and tumor-infiltrating leukocytes. | [107] |
| CyTOF | Dorsal root ganglia from C57/BL6 mice of both sexes | All samples were thawed, barcode labeled, and uniformly stained | NC | 50 species transition-metal elements and isotopes | A total of 30 molecularly distinct somatosensory glial and 41 distinct neuronal states across all time points in C57/BL6 mice of both sexes from embryonic day 11.5 to postnatal day 4 were quantified. | [108] |

NC: Not clear. ENPs: Engineered nanoparticles. NNPs: Natural nanoparticles.

3.2. SP-ICP-TOFMS Isotope Analysis

Specialized ICP-MS instruments such as the Multi-Collector ICP-MS (MC-ICP-MS) and ICP-TOFMS are used to measure accurate isotopic ratios [34,109]. MC-ICP-MS can provide high-precision isotopic ratios. Also, MC-ICP-MS has been shown to be capable of detecting multiple isotopes in single particles with an excellent accuracy [41,42,110].

Although MC-ICP-MS can measure a number of isotopes simultaneously, the m/z range and number of the isotopes are limited, which is depending on the number of the detectors installed on the instrument, making it difficult to apply to extensive elemental analysis. In addition, Faraday detectors on MC-ICP-MS instruments have a slow response time [110]. Consequently, the detector may not be able to detect the transient signals generated from NPs.

An advantage of SP-ICP-TOFMS over ICP-QMS is the ability to measure isotopic ratios in single particles. Tian et al. used several types of ICP-MS (ICP-QMS, ICP-TOFMS, and MC-ICP-MS) to simultaneously detect ¹⁰⁷Ag and ¹⁰⁹Ag in single AgNPs and single cyanobacterial cells exposed to AgNPs [104]. The results showed that ICP-QMS has a poor performance in isotope ratio analysis, but accurate silver ratios can be obtained by ICP-TOFMS and MC-ICP-MS. Compared to MC-ICP-MS, ICP-TOFMS can detect almost 100% paired events of single particles [104]. Bland et al. determined ⁴⁷Ti-enriched TiO₂ NPs in soil using SP-ICP-TOFMS and evaluated the tracking ability of isotope-enriched engineered NPs at the single particle level in soil [102]. The selected applications of SP-ICP-TOFMS in isotope ratio analysis of single particles are shown in Table 1.

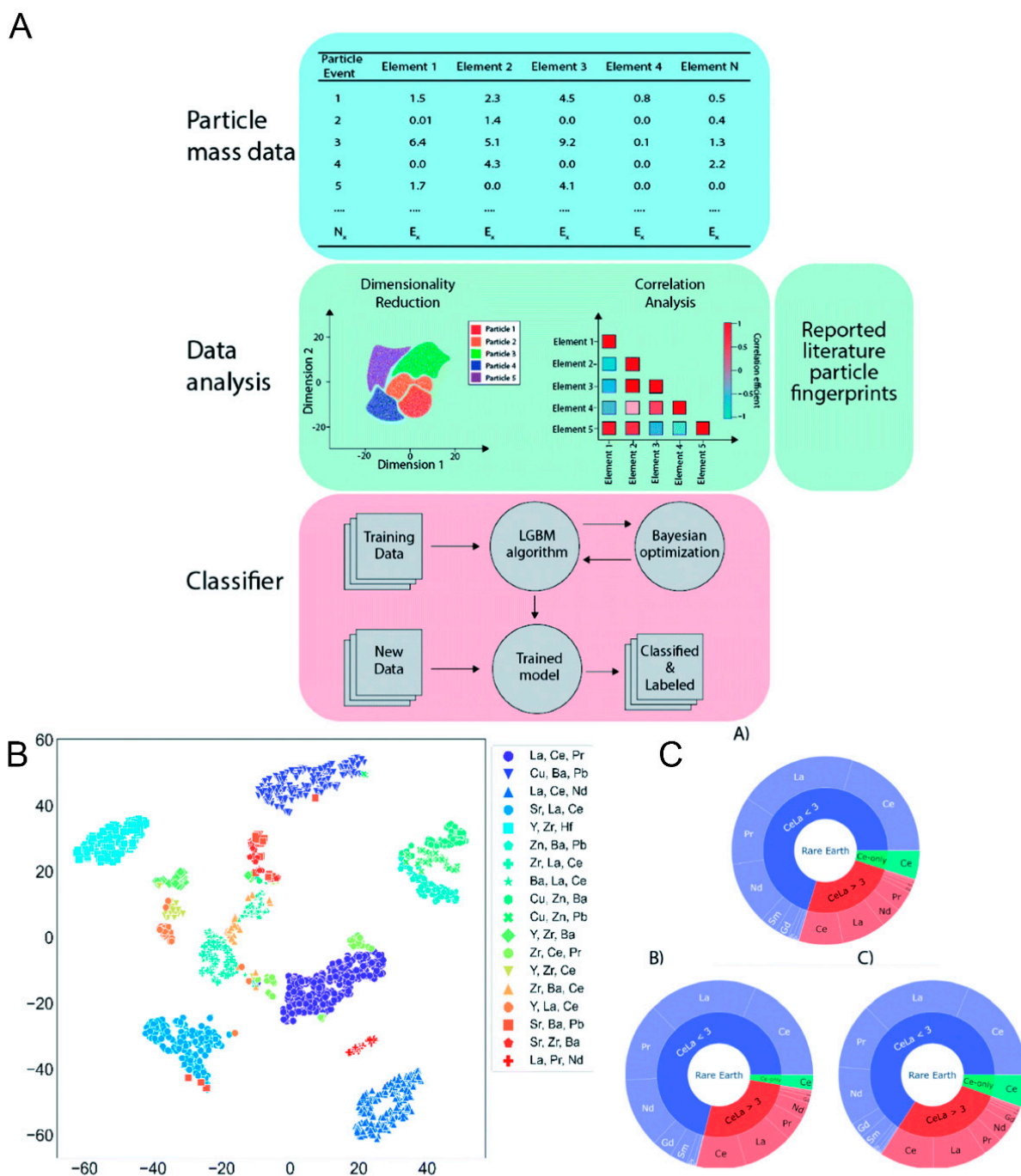


Figure 2. A machine learning model based on Pearson correlation and unsupervised T-distributed random neighbor embedding. **A.** Data analysis scheme for the multi-element particle analysis using dimensionality reduction (t-SNE), Pearson correlation analysis, and the creation of an automated LGBM classifier from particle mass data in combination with reported particle fingerprint markers. **B.** t-SNE plot of a sedimentation basin sample; the axis shows the dimension of the reduced dataset. The color and shape indicate specific particle types (i.e., purple circle: SrLaCe containing particles). **C.** Starburst plots of the particle counts of CeLa-containing particles and their associated elements. Class 1: CeLa containing particles (purple). Class 2: Ce containing particles with a Ce/La ratio greater than 3 (red). Class 3: Ce containing only cerium (green). Sample from (A) sedimentation basin, (B) road dust, and (C) tunnel road dust. (Reprinted with permission from Holbrook T. R J. *Anal. At. Spectrom.*, 2021, 36, 2684–2694. Copyright 2021, Royal Society of Chemistry [91]).

3.3. Single Cell (SC)-ICP-TOFMS

In recent years, single-cell analysis has become a growing field and has widely applied in biomedical research. Single-cell analysis is essential to reveal population heterogeneity, identify minority subpopulations of interest, and discover the unique characteristics of individual cells. Although several methods are available to analyze single cells, they are usually time-consuming and unable to detect elements in single cells [111,112]. Single cell-inductively coupled plasma-mass spectrometry (SC-ICP-MS) can be used to quantify elements in single cells. When ICP-TOFMS is used for single cell analysis, full mass spectrum can be obtained and there is no need to compromise on the analytes measured. All intrinsic elements in single cells can be measured, providing more insights into single cells [113]. This type of analysis does not require labeling or staining, as cells are detected based on their “native” elemental fingerprints [114]. Cell species can be distinguished by measuring elemental micronutrients unique to a particular cell type. For example, algal cells are rich in Mg [115], a core component of the chlorophyll pigment that is essential for photosynthesis. Therefore, the elemental composition can be used as a unique fingerprint to clearly identify different cell species.

Mass cytometry (CyTOF) is a recently developed method that combines ICP-TOFMS with flow cytometry [116–118]. This technology uses metal isotopes instead of fluorophores for antibodies labelling. Compared to traditional flow cytometry, the number of analytical channels in CyTOF is over 100 and the interference between adjacent channels is as low as ~0.1% [117], solving the problem of fluorescence crosstalk. CyTOF has the limitation on analytical throughput (~1000 events/s [119]) but provides more complex and multidimensional data than traditional flow cytometry. With the increasing demand for high throughput in bioanalytical research, it is critical to maximize the ability to produce information about multiple markers in a single run [120].

Currently, CyTOF allows for the simultaneous detection of up to 50 metal-isotope labels on a single cell [34]. Such highly multiparametric detection has provided new insights into the complexity of biology in applications ranging from the deep phenotyping of tumors to signaling pathways of the immune system [101,121]. Antibodies are mainly used as cell staining agents in CyTOF, which fails to detect most intrinsic elements (less than 75 Th) in single cells. Bendall et al. used labeled antibodies to bind to human bone marrow cells and simultaneously analyzed up to 34 different cell parameters by CyTOF [122]. Recently, Wen et al. explored the potential of ruthenium red as a stain for single-cell analysis [96], and ruthenium red allows the elemental content to be directly correlated with cell volume to accurately calculate the intracellular concentration of target elements in single cells. By measuring metal atoms at the cellular level, the fundamental biological processes regulated by metalloproteins and metalloenzymes can be better understood [123]. Table 1 also shows the selected application of CyTOF in single cell analysis.

4. Summary and Prospect

SP-ICP-TOFMS is a powerful analytical technique used for the characterization of NPs. Rapid advances in ICP-TOFMS instrumentation have made it possible to detect smaller NPs with greater efficiency and accuracy. The development of SP-ICP-TOFMS methodologies has also been successful in many research fields, allowing for the analysis of individual NPs with high sensitivity and specificity. SP-ICP-TOFMS is continuously evolving to overcome its current limitations and it is expected that new generations of ICP-TOFMS will further improve their ability to detect smaller NPs with better accuracy. Furthermore, the data processing for SP-ICP-TOFMS will become more automated with the development of advanced data processing programs. In addition, other analytical methods will also be coupled with SP-ICP-TOFMS to provide more comprehensive and useful information about NPs at the same time. As a result, it is expected that SP-ICP-TOFMS will continue to expand its applications and become a valuable tool in many fields, including nanotechnology, environmental science, and biomedicine.

Author Contributions: All authors actively contributed to manuscript drafting. Conceptualization: Z.M., M.W., L.Z. and W.F.; Writing—original draft: Z.M., L.Z. and M.W.; Literature survey: P.Y., H.F. and B.W.; Supervision: M.W., W.F. and L.L.; Writing—review and editing: Z.M., M.W., L.Z. and L.L. All authors have read and agreed to the published version of the manuscript.

Funding: The work is supported by Guangdong Basic and Applied Basic Research Fund (DG2231351B), the State Key Laboratory of Environmental Chemistry and Ecotoxicology (KF2020-19), and the Key Laboratory of Chemical Metrology and Applications on Nutrition and Health for State Market Regulation.

Data Availability Statement: The manuscript has no associated data.

Conflicts of Interest: The authors declare no conflict of interest.

References

1. Hochella, J.M.F.; Mogk, D.W.; Ranville, J.; Allen, I.C.; Luther, G.W.; Marr, L.C.; McGrail, B.P.; Murayama, M.; Qafoku, N.P.; Rosso, K.M.; et al. Natural, incidental, and engineered nanomaterials and their impacts on the Earth system. *Science* **2019**, *363*, eaau8299. [[CrossRef](#)] [[PubMed](#)]
2. Scott-Fordsmand, J.J.; Peijnenburg, W.J.G.M.; Semenzin, E.; Nowack, B.; Hunt, N.; Hristozov, D.; Marcomini, A.; Irfan, M.-A.; Jiménez, A.S.; Landsiedel, R.; et al. Environmental Risk Assessment Strategy for Nanomaterials. *Int. J. Environ. Res. Public Health* **2017**, *14*, 1251. [[CrossRef](#)] [[PubMed](#)]
3. Tiede, K.; Hassellöv, M.; Breitbarth, E.; Chaudhry, Q.; Boxall, A.B. Considerations for environmental fate and ecotoxicity testing to support environmental risk assessments for engineered nanoparticles. *J. Chromatogr. A* **2009**, *1216*, 503–509. [[CrossRef](#)] [[PubMed](#)]
4. Baun, A.; Hartmann, N.B.; Grieger, K.; Kusk, K.O. Ecotoxicity of engineered nanoparticles to aquatic invertebrates: A brief review and recommendations for future toxicity testing. *Ecotoxicology* **2008**, *17*, 387–395. [[CrossRef](#)]
5. Laborda, F.; Jiménez-Lamana, J.; Bolea, E.; Castillo, J.R. Critical considerations for the determination of nanoparticle number concentrations, size and number size distributions by single particle ICP-MS. *J. Anal. At. Spectrom.* **2013**, *28*, 1220–1232. [[CrossRef](#)]
6. Montaña, M.D.; Olesik, J.W.; Barber, A.G.; Challis, K.; Ranville, J.F. Single Particle ICP-MS: Advances toward routine analysis of nanomaterials. *Anal. Bioanal. Chem.* **2016**, *408*, 5053–5074. [[CrossRef](#)]
7. Mourdikoudis, S.; Pallares, R.M.; Thanh, N.T.K. Characterization techniques for nanoparticles: Comparison and complementarity upon studying nanoparticle properties. *Nanoscale* **2018**, *10*, 12871–12934. [[CrossRef](#)]
8. Meermann, B.; Nischwitz, V. ICP-MS for the analysis at the nanoscale—A tutorial review. *J. Anal. At. Spectrom.* **2018**, *33*, 1432–1468. [[CrossRef](#)]
9. Ammann, A.A. Inductively coupled plasma mass spectrometry (ICP MS): A versatile tool. *J. Mass. Spectrom.* **2007**, *42*, 419–427. [[CrossRef](#)]
10. Laborda, F.; Bolea, E.; Cepriá, G.; Gómez, M.T.; Jiménez, M.S.; Pérez-Arantegui, J.; Castillo, J.R. Detection, characterization and quantification of inorganic engineered nanomaterials: A review of techniques and methodological approaches for the analysis of complex samples. *Anal. Chim. Acta* **2016**, *904*, 10–32. [[CrossRef](#)]
11. Mitrano, D.M.; Leshner, E.K.; Bednar, A.; Monserud, J.; Higgins, C.P.; Ranville, J.F. Detecting nanoparticulate silver using single-particle inductively coupled plasma-mass spectrometry. *Environ. Toxicol. Chem.* **2012**, *31*, 115–121. [[CrossRef](#)]
12. Kawaguchi, H.; Fukasawa, N.; Mizuike, A. Investigation of airborne particles by inductively coupled plasma emission spectrometry calibrated with monodisperse aerosols. *Spectrochim. Acta Part B At. Spectrosc.* **1986**, *41*, 1277–1286. [[CrossRef](#)]
13. Nomizu, T.; Kaneco, S.; Tanaka, T.; Yamamoto, T.; Kawaguchi, H. Determination of Femto-gram Amounts of Zinc and Lead in Individual Airborne Particles by Inductively Coupled Plasma Mass Spectrometry with Direct Air-Sample Introduction. *Anal. Sci.* **1993**, *9*, 843–846. [[CrossRef](#)]
14. Degueldre, C.; Favarger, P.Y. Colloid analysis by single particle inductively coupled plasma-mass spectroscopy: A feasibility study. *Colloids Surf. A Physicochem. Eng. Asp.* **2003**, *217*, 137–142. [[CrossRef](#)]
15. Degueldre, C.; Favarger, P.Y. Thorium colloid analysis by single particle inductively coupled plasma-mass spectrometry. *Talanta* **2004**, *62*, 1051–1054. [[CrossRef](#)] [[PubMed](#)]
16. Degueldre, C.; Favarger, P.Y.; Bitea, C. Zirconia colloid analysis by single particle inductively coupled plasma-mass spectrometry. *Anal. Chim. Acta* **2004**, *518*, 137–142. [[CrossRef](#)]
17. Degueldre, C.; Favarger, P.Y.; Rossé, R.; Wold, S. Uranium colloid analysis by single particle inductively coupled plasma-mass spectrometry. *Talanta* **2006**, *68*, 623–628. [[CrossRef](#)] [[PubMed](#)]
18. Eiden, G.C.; Barinaga, C.J.; Koppenaal, D.W. Plasma source ion trap mass spectrometry: Enhanced abundance sensitivity by resonant ejection of atomic ions. *J. Am. Soc. Mass Spectrom.* **1996**, *7*, 1161–1171. [[CrossRef](#)]
19. Walder, A.J.; Freedman, P.A. Communication. Isotopic ratio measurement using a double focusing magnetic sector mass analyser with an inductively coupled plasma as an ion source. *J. Anal. At. Spectrom.* **1992**, *7*, 571–575. [[CrossRef](#)]
20. Balcaen, L.; Bolea-Fernandez, E.; Resano, M.; Vanhaecke, F. Inductively coupled plasma—Tandem mass spectrometry (ICP-MS/MS): A powerful and universal tool for the interference-free determination of (ultra)trace elements—A tutorial review. *Anal. Chim. Acta* **2015**, *894*, 7–19. [[CrossRef](#)]

21. Diez Fernández, S.; Sugishama, N.; Ruiz Encinar, J.; Sanz-Medel, A. Triple quad ICPMS (ICPQQQ) as a new tool for absolute quantitative proteomics and phosphoproteomics. *Anal. Chem.* **2012**, *84*, 5851–5857. [[CrossRef](#)] [[PubMed](#)]
22. Mozhayeva, D.; Engelhard, C. A critical review of single particle inductively coupled plasma mass spectrometry—A step towards an ideal method for nanomaterial characterization. *J. Anal. At. Spectrom.* **2020**, *35*, 1740–1783. [[CrossRef](#)]
23. Montaña, M.D.; Badieli, H.R.; Bazargan, S.; Ranville, J.F. Improvements in the detection and characterization of engineered nanoparticles using spICP-MS with microsecond dwell times. *Environ. Sci. Nano.* **2014**, *1*, 338–346. [[CrossRef](#)]
24. Loosli, F.; Wang, J.; Rothenberg, S.; Bizimis, M.; Winkler, C.; Borovinskaya, O.; Flamigni, L.; Baalousha, M. Sewage spills are a major source of titanium dioxide engineered (nano)-particle release into the environment. *Environ. Sci. Nano.* **2019**, *6*, 763–777. [[CrossRef](#)] [[PubMed](#)]
25. Wang, J.; Nabi, M.D.M.; Erfani, M.; Goharian, E.; Baalousha, M. Identification and quantification of anthropogenic nanomaterials in urban rain and runoff using single particle-inductively coupled plasma-time of flight-mass spectrometry. *Environ. Sci. Nano* **2022**, *9*, 714–729. [[CrossRef](#)]
26. Bland, G.D.; Battifarano, M.; Pradas del Real, A.E.; Sarret, G.; Lowry, G.V. Distinguishing Engineered TiO₂ Nanomaterials from Natural Ti Nanomaterials in Soil Using spICP-TOFMS and Machine Learning. *Environ. Sci. Technol.* **2022**, *56*, 2990–3001. [[CrossRef](#)]
27. Meili-Borovinskaya, O.; Meier, F.; Drexel, R.; Baalousha, M.; Flamigni, L.; Hegetschweiler, A.; Kraus, T. Analysis of complex particle mixtures by asymmetrical flow field-flow fractionation coupled to inductively coupled plasma time-of-flight mass spectrometry. *J. Chromatogr. A* **2021**, *1641*, 461981. [[CrossRef](#)]
28. Liu, Z.; Peng, R.; Lv, S.; Wang, A.; Zhao, L.; Dong, S.; Yan, D.; Keller, A.A.; Huang, Y. Evidence of indoor dust acting as carrier for metal-based nanoparticles: A study of exposure and oxidative risks. *Environ. Sci. Technol. Lett.* **2022**, *9*, 431–438. [[CrossRef](#)]
29. Borovinskaya, O.; Gschwind, S.; Hattendorf, B.; Tanner, M.; Günther, D. Simultaneous Mass Quantification of Nanoparticles of Different Composition in a Mixture by Microdroplet Generator-ICPTOFMS. *Anal. Chem.* **2014**, *86*, 8142–8148. [[CrossRef](#)] [[PubMed](#)]
30. Praetorius, A.; Gundlach-Graham, A.; Goldberg, E.; Fabienke, W.; Navratilova, J.; Gondikas, A.; Kaegi, R.; Günther, D.; Hofmann, T.; von der Kammer, F. Single-particle multi-element fingerprinting (spMEF) using inductively-coupled plasma time-of-flight mass spectrometry (ICP-TOFMS) to identify engineered nanoparticles against the elevated natural background in soils. *Environ. Sci. Nano.* **2017**, *4*, 307–314. [[CrossRef](#)]
31. Naasz, S.; Weigel, S.; Borovinskaya, O.; Serva, A.; Cascio, C.; Undas, A.K.; Simeone, F.C.; Marvin, H.J.P.; Peters, R.J.B. Multi-element analysis of single nanoparticles by ICP-MS using quadrupole and time-of-flight technologies. *J. Anal. At. Spectrom.* **2018**, *33*, 835–845. [[CrossRef](#)]
32. Montaña, M.D.; Cuss, C.W.; Holliday, H.M.; Javed, M.B.; Shoty, W.; Sobocinski, K.L.; Hofmann, T.; Kammer, F.v.d.; Ranville, J.F. Exploring Nanogeochemical Environments: New Insights from Single Particle ICP-TOFMS and AF4-ICPMS. *ACS Earth Space Chem.* **2022**, *6*, 943–952. [[CrossRef](#)]
33. Myers, D.P.; Hieftje, G.M. Preliminary Design Considerations and Characteristics of an Inductively Coupled Plasma-Time-of-Flight Mass Spectrometer. *Microchem. J.* **1993**, *48*, 259–277. [[CrossRef](#)]
34. Hendriks, L.; Gundlach-Graham, A.; Hattendorf, B.; Günther, D. Characterization of a new ICP-TOFMS instrument with continuous and discrete introduction of solutions. *J. Anal. At. Spectrom.* **2017**, *32*, 548–561. [[CrossRef](#)]
35. Borovinskaya, O.; Hattendorf, B.; Tanner, M.; Gschwind, S.; Günther, D. A prototype of a new inductively coupled plasma time-of-flight mass spectrometer providing temporally resolved, multi-element detection of short signals generated by single particles and droplets. *J. Anal. At. Spectrom.* **2013**, *28*, 226–233. [[CrossRef](#)]
36. Hong, A.; Tang, Q.; Khan, A.U.; Miao, M.; Xu, Z.; Dang, F.; Liu, Q.; Wang, Y.; Lin, D.; Filser, J.; et al. Identification and Speciation of Nanoscale Silver in Complex Solid Matrices by Sequential Extraction Coupled with Inductively Coupled Plasma Optical Emission Spectrometry. *Anal. Chem.* **2021**, *93*, 1962–1968. [[CrossRef](#)]
37. Ji, X.; Yang, L.; Wu, F.; Yao, L.; Yu, B.; Liu, X.; Yin, Y.; Hu, L.; Qu, G.; Fu, J.; et al. Identification of mercury-containing nanoparticles in the liver and muscle of cetaceans. *J. Hazard. Mater.* **2022**, *424*, 127759. [[CrossRef](#)]
38. Jiang, M.; Zhou, J.; Xie, X.; Huang, Z.; Liu, R.; Lv, Y. Single nanoparticle counting-based liquid biopsy for cancer diagnosis. *Anal. Chem.* **2022**, *94*, 15433–15439. [[CrossRef](#)]
39. Hineman, A.; Stephan, C. Effect of dwell time on single particle inductively coupled plasma mass spectrometry data acquisition quality. *J. Anal. At. Spectrom.* **2014**, *29*, 1252–1257. [[CrossRef](#)]
40. Chun, K.H.; Lum, J.T.; Leung, K.S. Dual-elemental analysis of single particles using quadrupole-based inductively coupled plasma-mass spectrometry. *Anal. Chim. Acta* **2022**, *1192*, 339389. [[CrossRef](#)]
41. Su, Y.; Wang, W.; Li, Z.; Deng, H.; Zhou, G.; Xu, J.; Ren, X. Direct detection and isotope analysis of individual particles in suspension by single particle mode MC-ICP-MS for nuclear safety. *J. Anal. At. Spectrom.* **2015**, *30*, 1184–1190. [[CrossRef](#)]
42. Yamashita, S.; Ishida, M.; Suzuki, T.; Nakazato, M.; Hirata, T. Isotopic analysis of platinum from single nanoparticles using a high-time resolution multiple collector Inductively Coupled Plasma—Mass Spectroscopy. *Spectrochim. Acta Part B At. Spectrosc.* **2020**, *169*, 105881. [[CrossRef](#)]
43. Gundlach-Graham, A. *Multiplexed and Multi-Metal Single-Particle Characterization with ICP-TOFMS*; Milačič, R., Ščančar, J., Goenaga-Infante, H., Vidmar, J., Eds.; Elsevier: Cambridge, MA, USA, 2021; Volume 93, pp. 69–101. ISBN 9780323853057.

44. Chang, P.-P.; Zheng, L.-N.; Wang, B.; Chen, M.-L.; Wang, M.; Wang, J.-H.; Feng, W.-Y. ICP-MS-Based Methodology in Metallomics: Towards Single Particle Analysis, Single Cell Analysis, and Spatial Metallomics. *At. Spectrosc.* **2022**, *43*, 255–265. [[CrossRef](#)]
45. Resano, M.; Aramendía, M.; García-Ruiz, E.; Bazo, A.; Bolea-Fernandez, E.; Vanhaecke, F. Living in a transient world: ICP-MS reinvented via time-resolved analysis for monitoring single events. *Chem. Sci.* **2022**, *13*, 4436–4473. [[CrossRef](#)] [[PubMed](#)]
46. Sharp, B.L. Pneumatic nebulisers and spray chambers for inductively coupled plasma spectrometry. A review. Part 1. Nebulisers. *J. Anal. At. Spectrom.* **1988**, *3*, 613–652. [[CrossRef](#)]
47. Lamsal, R.P.; Hineman, A.; Stephan, C.; Tahmasebi, S.; Baranton, S.; Coutanceau, C.; Jerkiewicz, G.; Beauchemin, D. Characterization of platinum nanoparticles for fuel cell applications by single particle inductively coupled plasma mass spectrometry. *Anal. Chim. Acta* **2020**, *1139*, 36–41. [[CrossRef](#)]
48. Tharaud, M.; Louvat, P.; Benedetti, M.F. Detection of nanoparticles by single-particle ICP-MS with complete transport efficiency through direct nebulization at few-microlitres-per-minute uptake rates. *Anal. Bioanal. Chem.* **2021**, *413*, 923–933. [[CrossRef](#)]
49. Gundlach-Graham, A.; Mehrabi, K. Monodisperse microdroplets: A tool that advances single-particle ICP-MS measurements. *J. Anal. At. Spectrom.* **2020**, *35*, 1727–1739. [[CrossRef](#)]
50. Verboket, P.E.; Borovinskaya, O.; Meyer, N.; Günther, D.; Dittrich, P.S. A new microfluidics-based droplet dispenser for ICPMS. *Anal. Chem.* **2014**, *86*, 6012–6018. [[CrossRef](#)]
51. Hendriks, L.; Ramkorun-Schmidt, B.; Gundlach-Graham, A.; Koch, J.; Grass, R.N.; Jakubowski, N.; Günther, D. Single-particle ICP-MS with online microdroplet calibration: Toward matrix independent nanoparticle sizing. *J. Anal. At. Spectrom.* **2019**, *34*, 716–728. [[CrossRef](#)]
52. Metarapi, D.; van Elteren, J.T.; Šala, M.; Vogel-Mikuš, K.; Arčon, I.; Šelih, V.S.; Kolar, M.; Hočevar, S.B. Laser ablation-single-particle-inductively coupled plasma mass spectrometry as a multimodality bioimaging tool in nano-based omics. *Environ. Sci. Nano.* **2021**, *8*, 647–656. [[CrossRef](#)]
53. Wang, M.; Zheng, L.; Wang, B.; Yang, P.; Fang, H.; Liang, S.; Chen, W.; Feng, W. Laser ablation-single particle-inductively coupled plasma mass spectrometry as a sensitive tool for bioimaging of silver nanoparticles in vivo degradation. *Chin. Chem. Lett.* **2022**, *33*, 3484–3487. [[CrossRef](#)]
54. Geertsen, V.; Barruet, E.; Gobeaux, F.; Lacour, J.-L.; Taché, O. Contribution to Accurate Spherical Gold Nanoparticle Size Determination by Single-Particle Inductively Coupled Mass Spectrometry: A Comparison with Small-Angle X-ray Scattering. *Anal. Chem.* **2018**, *90*, 9742–9750. [[CrossRef](#)] [[PubMed](#)]
55. Abad-Alvaro, I.; Pena-Vazquez, E.; Bolea, E.; Bermejo-Barrera, P.; Castillo, J.R.; Laborda, F. Evaluation of number concentration quantification by single-particle inductively coupled plasma mass spectrometry: Microsecond vs. millisecond dwell times. *Anal. Bioanal. Chem.* **2016**, *408*, 5089–5097. [[CrossRef](#)] [[PubMed](#)]
56. Laborda, F.; Bolea, E.; Jimenez-Lamana, J. Single particle inductively coupled plasma mass spectrometry: A powerful tool for nanoanalysis. *Anal. Chem.* **2014**, *86*, 2270–2278. [[CrossRef](#)] [[PubMed](#)]
57. Pace, H.E.; Rogers, N.J.; Jarolimek, C.; Coleman, V.A.; Higgins, C.P.; Ranville, J.F. Determining transport efficiency for the purpose of counting and sizing nanoparticles via single particle inductively coupled plasma mass spectrometry. *Anal. Chem.* **2011**, *83*, 9361–9369. [[CrossRef](#)]
58. Laborda, F.; Gimenez-Ingalaturre, A.C.; Bolea, E.; Castillo, J.R. About detectability and limits of detection in single particle inductively coupled plasma mass spectrometry. *Spectrochim. Acta Part B At. Spectrosc.* **2020**, *169*, 105883. [[CrossRef](#)]
59. Lee, S.; Bi, X.; Reed, R.B.; Ranville, J.F.; Herckes, P.; Westerhoff, P. Nanoparticle size detection limits by single particle ICP-MS for 40 elements. *Environ. Sci. Technol.* **2014**, *48*, 10291–10300. [[CrossRef](#)]
60. Vidmar, J.; Milačič, R.; Ščančar, J. Sizing and simultaneous quantification of nanoscale titanium dioxide and a dissolved titanium form by single particle inductively coupled plasma mass spectrometry. *Microchem. J.* **2017**, *132*, 391–400. [[CrossRef](#)]
61. Tuoriniemi, J.; Cornelis, G.; Hassellöv, M. A new peak recognition algorithm for detection of ultra-small nano-particles by single particle ICP-MS using rapid time resolved data acquisition on a sector-field mass spectrometer. *J. Anal. At. Spectrom.* **2015**, *30*, 1723–1729. [[CrossRef](#)]
62. Laborda, F.; Gimenez-Ingalaturre, A.C.; Bolea, E.; Castillo, J.R. Single particle inductively coupled plasma mass spectrometry as screening tool for detection of particles. *Spectrochim. Acta Part B At. Spectrosc.* **2019**, *159*, 105654. [[CrossRef](#)]
63. Currie, L.A. Limits for qualitative detection and quantitative determination. Application to radiochemistry. *Anal. Chem.* **1968**, *40*, 586–593. [[CrossRef](#)]
64. Currie, L.A. Nomenclature in evaluation of analytical methods including detection and quantification capabilities (IUPAC Recommendations 1995). *Pure Appl. Chem.* **1995**, *67*, 1699–1723. [[CrossRef](#)]
65. Gundlach-Graham, A.; Hendriks, L.; Mehrabi, K.; Gunther, D. Monte Carlo Simulation of Low-Count Signals in Time-of-Flight Mass Spectrometry and Its Application to Single-Particle Detection. *Anal. Chem.* **2018**, *90*, 11847–11855. [[CrossRef](#)] [[PubMed](#)]
66. Hendriks, L.; Gundlach-Graham, A.; Günther, D. Performance of sp-ICP-TOFMS with signal distributions fitted to a compound Poisson model. *J. Anal. At. Spectrom.* **2019**, *34*, 1900–1909. [[CrossRef](#)]
67. Huang, Y.; Tsz-Shan Lum, J.; Sze-Yin Leung, K. Single particle ICP-MS combined with internal standardization for accurate characterization of polydisperse nanoparticles in complex matrices. *J. Anal. At. Spectrom.* **2020**, *35*, 2148–2155. [[CrossRef](#)]
68. Gschwind, S.; Flamigni, L.; Koch, J.; Borovinskaya, O.; Groh, S.; Niemax, K.; Gunther, D. Capabilities of inductively coupled plasma mass spectrometry for the detection of nanoparticles carried by monodisperse microdroplets. *J. Anal. At. Spectrom.* **2011**, *26*, 1166–1174. [[CrossRef](#)]

69. Koch, J.; Flamigni, L.; Gschwind, S.; Allner, S.; Longerich, H.; Günther, D. Accelerated evaporation of microdroplets at ambient conditions for the on-line analysis of nanoparticles by inductively-coupled plasma mass spectrometry. *J. Anal. At. Spectrom.* **2013**, *28*, 1669–1806. [[CrossRef](#)]
70. Mehrabi, K.; Günther, D.; Gundlach-Graham, A. Single-particle ICP-TOFMS with online microdroplet calibration for the simultaneous quantification of diverse nanoparticles in complex matrices. *Environ. Sci. Nano.* **2019**, *6*, 3349–3358. [[CrossRef](#)]
71. Hendriks, L.; Gundlach-Graham, A.; Günther, D. Analysis of Inorganic Nanoparticles by Single-particle Inductively Coupled Plasma Time-of-Flight Mass Spectrometry. *Chimia* **2018**, *72*, 221–226. [[CrossRef](#)]
72. Harycki, S.; Gundlach-Graham, A. Online microdroplet calibration for accurate nanoparticle quantification in organic matrices. *Anal. Bioanal. Chem.* **2022**, *414*, 7543–7551. [[CrossRef](#)]
73. Flores, K.; Turley, R.S.; Valdes, C.; Ye, Y.; Cantu, J.; Hernandez-Viezcas, J.A.; Parsons, J.G.; Gardea-Torresdey, J.L. Environmental applications and recent innovations in single particle inductively coupled plasma mass spectrometry (SP-ICP-MS). *Appl. Spectrosc. Rev.* **2019**, *56*, 1–26. [[CrossRef](#)]
74. Klaine, S.J.; Koelmans, A.A.; Horne, N.; Carley, S.; Handy, R.D.; Kapustka, L.; Nowack, B.; von der Kammer, F. Paradigms to assess the environmental impact of manufactured nanomaterials. *Environ. Toxicol. Chem.* **2012**, *31*, 3–14. [[CrossRef](#)]
75. Nowack, B.; Boldrin, A.; Caballero, A.; Hansen, S.F.; Gottschalk, F.; Heggelund, L.; Hennig, M.; Mackevica, A.; Maes, H.; Navratilova, J.; et al. Meeting the Needs for Released Nanomaterials Required for Further Testing—The SUN Approach. *Environ. Sci. Technol.* **2016**, *50*, 2747–2753. [[CrossRef](#)] [[PubMed](#)]
76. Zhang, M.; Yang, J.; Cai, Z.; Feng, Y.; Wang, Y.; Zhang, D.; Pan, X. Detection of engineered nanoparticles in aquatic environments: Current status and challenges in enrichment, separation, and analysis. *Environ. Sci. Nano.* **2019**, *6*, 709–735. [[CrossRef](#)]
77. Qi, J.; Lai, X.; Wang, J.; Tang, H.; Ren, H.; Yang, Y.; Jin, Q.; Zhang, L.; Yu, R.; Ma, G.; et al. Multi-shelled hollow micro-/nanostructures. *Chem. Soc. Rev.* **2015**, *44*, 6749–6773. [[CrossRef](#)]
78. Strobel, R.; Metz, H.; Pratsinis, S. Brilliant Yellow, Transparent Pure, and SiO₂-Coated BiVO₄ Nanoparticles Made in Flames. *Chem. Mater.* **2008**, *20*, 6346–6351. [[CrossRef](#)]
79. Erhardt, T.; Jensen, C.M.; Borovinskaya, O.; Fischer, H. Single Particle Characterization and Total Elemental Concentration Measurements in Polar Ice Using Continuous Flow Analysis-Inductively Coupled Plasma Time-of-Flight Mass Spectrometry. *Environ. Sci. Technol.* **2019**, *53*, 13275–13283. [[CrossRef](#)] [[PubMed](#)]
80. Tou, F.; Nabi, M.M.; Wang, J.; Erfani, M.; Goharian, E.; Chen, J.; Yang, Y.; Baalousha, M. Multi-method approach for analysis of road dust particles: Elemental ratios, SP-ICP-TOF-MS, and TEM. *Environ. Sci. Nano.* **2022**, *9*, 3859–3872. [[CrossRef](#)]
81. Jahn, L.G.; Bland, G.D.; Monroe, L.W.; Sullivan, R.C.; Meyer, M.E. Single-particle elemental analysis of vacuum bag dust samples collected from the International Space Station by SEM/EDX and sp-ICP-ToF-MS. *Aerosol Sci. Technol.* **2021**, *55*, 571–585. [[CrossRef](#)]
82. Jahn, L.G.; Jahl, L.G.; Bland, G.D.; Bowers, B.B.; Monroe, L.W.; Sullivan, R.C. Metallic and crustal elements in biomass-burning aerosol and ash: Prevalence, significance, and similarity to soil particles. *ACS Earth Space Chem.* **2021**, *5*, 136–148. [[CrossRef](#)]
83. Mehrabi, K.; Kaegi, R.; Günther, D.; Gundlach-Graham, A. Quantification and Clustering of Inorganic Nanoparticles in Wastewater Treatment Plants across Switzerland. *Chimia* **2021**, *75*, 642–646. [[CrossRef](#)] [[PubMed](#)]
84. Nabi, M.M.; Wang, J.; Baalousha, M. Episodic surges in titanium dioxide engineered particle concentrations in surface waters following rainfall events. *Chemosphere* **2021**, *263*, 128261. [[CrossRef](#)] [[PubMed](#)]
85. Mehrabi, K.; Dengler, M.; Nilsson, I.; Baumgartner, M.; Mora, C.A.; Günther, D.; Gundlach-Graham, A. Detection of magnetic iron nanoparticles by single-particle ICP-TOFMS: Case study for a magnetic filtration medical device. *Anal. Bioanal. Chem.* **2022**, *414*, 6743–6751. [[CrossRef](#)] [[PubMed](#)]
86. Szakas, S.E.; Lancaster, R.; Kaegi, R.; Gundlach-Graham, A. Quantification and classification of engineered, incidental, and natural cerium-containing particles by spICP-TOFMS. *Environ. Sci. Nano.* **2022**, *9*, 1627–1638. [[CrossRef](#)]
87. Hagino, H.; Tonegawa, Y.; Tanner, M.; Borovinskaya, O.; Hikita, T.; Shimono, A. Application of ICP-TOFMS for Real-Time Measurement of Trace Elements in Automotive Exhaust Particulate Matters from Engine Oil Additives. *Trans. Soc. Automot. Eng. Jpn.* **2017**, *48*, 1341–1346. [[CrossRef](#)]
88. Baalousha, M.; Wang, J.; Erfani, M.; Goharian, E. Elemental fingerprints in natural nanomaterials determined using SP-ICP-TOF-MS and clustering analysis. *Sci. Total Environ.* **2021**, *792*, 148426. [[CrossRef](#)]
89. Goodman, A.J.; Gundlach-Graham, A.; Bevers, S.G.; Ranville, J.F. Characterization of nano-scale mineral dust aerosols in snow by single particle inductively coupled plasma mass spectrometry. *Environ. Sci. Nano.* **2022**, *9*, 2638–2652. [[CrossRef](#)]
90. Mehrabi, K.; Kaegi, R.; Günther, D.; Gundlach-Graham, A. Emerging investigator series: Automated single-nanoparticle quantification and classification: A holistic study of particles into and out of wastewater treatment plants in Switzerland. *Environ. Sci. Nano.* **2021**, *8*, 1211–1225. [[CrossRef](#)]
91. Holbrook, T.R.; Gallot-Duval, D.; Reemtsma, T.; Wagner, S. Machine learning: Our future spotlight into single-particle ICP-ToF-MS analysis. *J. Anal. At. Spectrom.* **2021**, *36*, 2684–2694. [[CrossRef](#)]
92. Gondikas, A.; von der Kammer, F.; Kaegi, R.; Borovinskaya, O.; Neubauer, E.; Navratilova, J.; Praetorius, A.; Cornelis, G.; Hofmann, T. Where is the nano? Analytical approaches for the detection and quantification of TiO₂ engineered nanoparticles in surface waters. *Environ. Sci. Nano.* **2018**, *5*, 313–326. [[CrossRef](#)]
93. Hegetschweiler, A.; Borovinskaya, O.; Staudt, T.; Kraus, T. Single-Particle Mass Spectrometry of Titanium and Niobium Carbonitride Precipitates in Steels. *Anal. Chem.* **2019**, *91*, 943–950. [[CrossRef](#)]

94. Bevers, S.; Montañó, M.D.; Rybicki, L.; Hofmann, T.; von der Kammer, F.; Ranville, J.F. Quantification and Characterization of Nanoparticulate Zinc in an Urban Watershed. *Front. Environ. Sci.* **2020**, *8*, 84. [[CrossRef](#)]
95. Azimzada, A.; Farner, J.M.; Jreije, I.; Hadioui, M.; Liu-Kang, C.; Tufenkji, N.; Shaw, P.; Wilkinson, K.J. Single- and Multi-Element Quantification and Characterization of TiO₂ Nanoparticles Released From Outdoor Stains and Paints. *Front. Environ. Sci.* **2020**, *8*, 91. [[CrossRef](#)]
96. Win, Q.; Stärk, H.-J.; Reemtsma, T. Ruthenium red: A highly efficient and versatile cell staining agent for single-cell analysis using inductively coupled plasma time-of-flight mass spectrometry. *Analyst* **2021**, *146*, 6753–6759. [[CrossRef](#)]
97. Azimzada, A.; Jreije, I.; Hadioui, M.; Shaw, P.; Farner, J.M.; Wilkinson, K.J. Quantification and Characterization of Ti-, Ce-, and Ag-Nanoparticles in Global Surface Waters and Precipitation. *Environ. Sci. Technol.* **2021**, *55*, 9836–9844. [[CrossRef](#)] [[PubMed](#)]
98. von der Au, M.; Faßbender, S.; Chronakis, M.I.; Vogl, J.; Meermann, B. Size determination of nanoparticles by ICP-ToF-MS using isotope dilution in microdroplets. *J. Anal. At. Spectrom.* **2022**, *37*, 1203–1207. [[CrossRef](#)]
99. Bland, G.D.; Zhang, P.; Valsami-Jones, E.; Lowry, G.V. Application of Isotopically Labeled Engineered Nanomaterials for Detection and Quantification in Soils via Single-Particle Inductively Coupled Plasma Time-of-Flight Mass Spectrometry. *Environ. Sci. Technol.* **2022**, *56*, 15584–15593. [[CrossRef](#)]
100. Brünjes, R.; Schürman, J.; Kammer, F.v.d.; Hofmann, T. Rapid analysis of gunshot residues with single-particle inductively coupled plasma time-of-flight mass spectrometry. *Forensic Sci. Int.* **2022**, *332*, 111202. [[CrossRef](#)]
101. Harycki, S.; Gundlach-Graham, A. Characterization of a high-sensitivity ICP-TOFMS instrument for microdroplet, nanoparticle, and microplastic analyses. *J. Anal. At. Spectrom.* **2023**, *38*, 111–120. [[CrossRef](#)]
102. Koolen, C.D.; Torrent, L.; Agarwal, A.; Meili-Borovinskaya, O.; Gasilova, N.; Li, M.; Luo, W.; Züttel, A. High-Throughput Sizing, Counting, and Elemental Analysis of Anisotropic Multimetallic Nanoparticles with Single-Particle Inductively Coupled Plasma Mass Spectrometry. *ACS Nano* **2022**, *16*, 11968–11978. [[CrossRef](#)]
103. Taskula, S.; Stetten, L.; von der Kammer, F.; Hofmann, T. Platinum Nanoparticle Extraction, Quantification, and Characterization in Sediments by Single-Particle Inductively Coupled Plasma Time-of-Flight Mass Spectrometry. *Nanomaterials* **2022**, *12*, 3307. [[CrossRef](#)]
104. Tian, X.; Jiang, H.; Wang, M.; Cui, W.; Guo, Y.; Zheng, L.; Hu, L.; Qu, G.; Yin, Y.; Cai, Y.; et al. Exploring the performance of quadrupole, time-of-flight, and multi-collector ICP-MS for dual-isotope detection on single nanoparticles and cells. *Anal. Chim. Acta* **2023**, *1240*, 340756. [[CrossRef](#)] [[PubMed](#)]
105. Chronakis, M.I.; von der Au, M.; Meermann, B. Single cell-asymmetrical flow field-flow fractionation/ICP-time of flight-mass spectrometry (sc-AF4/ICP-ToF-MS): An efficient alternative for the cleaning and multielemental analysis of individual cells. *J. Anal. At. Spectrom.* **2022**, *37*, 2691–2700. [[CrossRef](#)]
106. Yoshida, Y.; Yoshio, S.; Yamazoe, T.; Mori, T.; Tsustui, Y.; Kawai, H.; Yoshikawa, S.; Fukuhara, T.; Okamoto, T.; Ono, Y.; et al. Phenotypic Characterization by Single-Cell Mass Cytometry of Human Intrahepatic and Peripheral NK Cells in Patients with Hepatocellular Carcinoma. *Cells* **2021**, *10*, 1495. [[CrossRef](#)] [[PubMed](#)]
107. Hartmann, F.J.; Simonds, E.F.; Bendall, S.C. A Universal Live Cell Barcoding-Platform for Multiplexed Human Single Cell Analysis. *Sci. Rep.* **2018**, *8*, 10770. [[CrossRef](#)] [[PubMed](#)]
108. Keeler, A.B.; Van Deusen, A.L.; Gadani, I.C.; Williams, C.M.; Goggin, S.M.; Hirt, A.K.; Vradenburgh, S.A.; Fread, K.I.; Puleo, E.A.; Jin, L.; et al. A developmental atlas of somatosensory diversification and maturation in the dorsal root ganglia by single-cell mass cytometry. *Nat. Neurosci.* **2022**, *25*, 1543–1558. [[CrossRef](#)]
109. Ohata, M.; Hagino, H. Examination on simultaneous multi-element isotope ratio measurement by inductively coupled plasma time of flight mass spectrometry. *Int. J. Mass. Spectrom.* **2018**, *430*, 31–36. [[CrossRef](#)]
110. Yamashita, S.; Yamamoto, K.; Takahashi, H.; Hirata, T. Size and isotopic ratio measurements of individual nanoparticles by a continuous ion-monitoring method using Faraday detectors equipped on a multi-collector-ICP-mass spectrometer. *J. Anal. At. Spectrom.* **2022**, *37*, 178–184. [[CrossRef](#)]
111. Brandenberger, C.; Clift, M.J.; Vanhecke, D.; Mühlfeld, C.; Stone, V.; Gehr, P.; Rothen-Rutishauser, B. Intracellular imaging of nanoparticles: Is it an elemental mistake to believe what you see? *Part. Fibre Toxicol.* **2010**, *7*, 15. [[CrossRef](#)]
112. Jensen, L.H.S.; Skjolding, L.M.; Thit, A.; Sørensen, S.N.; Købler, C.; Mølhav, K.; Baun, A. Not all that glitters is gold—Electron microscopy study on uptake of gold nanoparticles in *Daphnia magna* and related artifacts. *Environ. Toxicol. Chem.* **2017**, *36*, 1503–1509. [[CrossRef](#)]
113. Hendriks, L.; Skjolding, L.M.; Thomas, R. Single-Cell Analysis by Inductively Coupled Plasma–Time-of-Flight Mass Spectrometry to Quantify Algal Cell Interaction with Nanoparticles by Their Elemental Fingerprint. *Spectroscopy* **2020**, *35*, 9–16.
114. von der Au, M.; Borovinskaya, O.; Flamigni, L.; Kuhlmeier, K.; Büchel, C.; Meermann, B. Single cell-inductively coupled plasma-time of flight-mass spectrometry approach for ecotoxicological testing. *Algal Res.* **2020**, *49*, 101964. [[CrossRef](#)]
115. Markou, G.; Vandamme, D.; Muylaert, K. Microalgal and cyanobacterial cultivation: The supply of nutrients. *Water Res.* **2014**, *65*, 186–202. [[CrossRef](#)] [[PubMed](#)]
116. Tracey, L.J.; An, Y.; Justice, M.J. CyTOF: An Emerging Technology for Single-Cell Proteomics in the Mouse. *Curr. Protoc.* **2021**, *1*, e118. [[CrossRef](#)]
117. Bandura, D.R.; Baranov, V.I.; Ornatsky, O.I.; Antonov, A.; Kinach, R.; Lou, X.; Pavlov, S.; Vorobiev, S.; Dick, J.E.; Tanner, S.D. Mass Cytometry: Technique for Real Time Single Cell Multitarget Immunoassay Based on Inductively Coupled Plasma Time-of-Flight Mass Spectrometry. *Anal. Chem.* **2009**, *81*, 6813–6822. [[CrossRef](#)]

118. Bendall, S.C.; Simonds, E.F.; Qiu, P.; Amir, E.-a.D.; Krutzik, P.O.; Finck, R.; Bruggner, R.V.; Melamed, R.; Trejo, A.; Ornatsky, O.I.; et al. Single-Cell Mass Cytometry of Differential Immune and Drug Responses Across a Human Hematopoietic Continuum. *Science* **2011**, *332*, 687–696. [[CrossRef](#)]
119. Hiramatsu, K.; Ideguchi, T.; Yonamine, Y.; Lee, S.; Luo, Y.; Hashimoto, K.; Ito, T.; Hase, M.; Park, J.W.; Kasai, Y.; et al. High-throughput label-free molecular fingerprinting flow cytometry. *Sci. Adv.* **2019**, *5*, eaau0241. [[CrossRef](#)]
120. Nassar, A.F.; Wisnewski, A.V.; Raddassi, K. Mass cytometry moving forward in support of clinical research: Advantages and considerations. *Bioanalysis* **2016**, *8*, 255–257. [[CrossRef](#)]
121. Bendall, S.C.; Nolan, G.P. From single cells to deep phenotypes in cancer. *Nat. Biotechnol.* **2012**, *30*, 639–647. [[CrossRef](#)]
122. Bendall, S.C.; Nolan, G.P.; Roederer, M.; Chattopadhyay, P.K. A deep profiler's guide to cytometry. *Trends Immunol.* **2012**, *33*, 323–332. [[CrossRef](#)] [[PubMed](#)]
123. Mueller, L.P.; Traub, H.; Jakubowski, N.; Drescher, D.; Baranov, V.I.; Kneipp, J. Trends in single-cell analysis by use of ICP-MS. *Anal. Bioanal. Chem.* **2014**, *406*, 6963–6977. [[CrossRef](#)] [[PubMed](#)]

Disclaimer/Publisher's Note: The statements, opinions and data contained in all publications are solely those of the individual author(s) and contributor(s) and not of MDPI and/or the editor(s). MDPI and/or the editor(s) disclaim responsibility for any injury to people or property resulting from any ideas, methods, instructions or products referred to in the content.